Short Range Correlations in Medium- and High-Energy Scattering off Nuclei

M. Alvioli*, C. Ciofi degli Atti,*, C. B. Mezzetti*, V. Palli*, S. Scopetta*, L. P. Kaptari† and H. Morita**

*Department of Physics, University of Perugia and Istituto Nazionale di Fisica Nucleare, Sezione di Perugia, Via A. Pascoli, I-06123, Italy
†Bogoliubov Laboratory of Theoretical Physics,141980, JINR, Dubna, Russia
**Sapporo Gakuin University, Bunkyo-dai 11, Ebetsu 069, Hokkaido, Japan

Abstract. The effects of short range correlations in lepton and hadron scattering off nuclei at medium and high energies are discussed.

Keywords: short-range correlations, particle-nucleus scattering
PACS: 24.10.Cn,25.30.-c,25.40.-h

INTRODUCTION

There is at present an uprise of interest in the longstanding problem concerning the role played by Nucleon-Nucleon (NN) short range correlations (SRC) in medium and high energy scattering off nuclei thanks particularly to the results of a series of dedicated experiments providing quantitative information on proton-neutron (p-n) and proton-proton (p-p) SRC in nuclei [1]. In view of these results, as well as of previous demonstrations of the inadequacy of the mean field picture of nuclei to describe the high momentum behavior of the nuclear wave functions (see e.g. [2]), it is timely to carefully analyze the effects of SRC in various scattering processes, paying particular attention to those competing effects, particularly final state interaction (FSI) effects, which make the study of SRC not easy task. In what follows the results of several calculations performed at the University of Perugia along this line will be presented.

THE A(e, e′p)B PROCESS IN FEW-NUCLEON SYSTEMS

Exclusive lepton scattering off nuclei $A(e,e'p)B$ in the quasi elastic region, plays a relevant role in nowadays hadronic physics, since it can provide information on: i) SRC; ii) the details of the mechanism of propagation of hadronic states in the medium; iii) QCD predictions like, e.g., color transparency effects. At medium and high energies the propagation of a struck hadron in the medium is usually treated within the Glauber multiple scattering approach (GA), which has been applied with great success to hadron scattering off nuclear targets. However, when the hadron is created inside the nucleus various improvements of the original GA have been advocated; worth being mentioned is the generalized eikonal approximation (GEA) [3] where, unlike GA, the excitation energy of the $A-1$ system is partly taken into account. The GEA has recently been

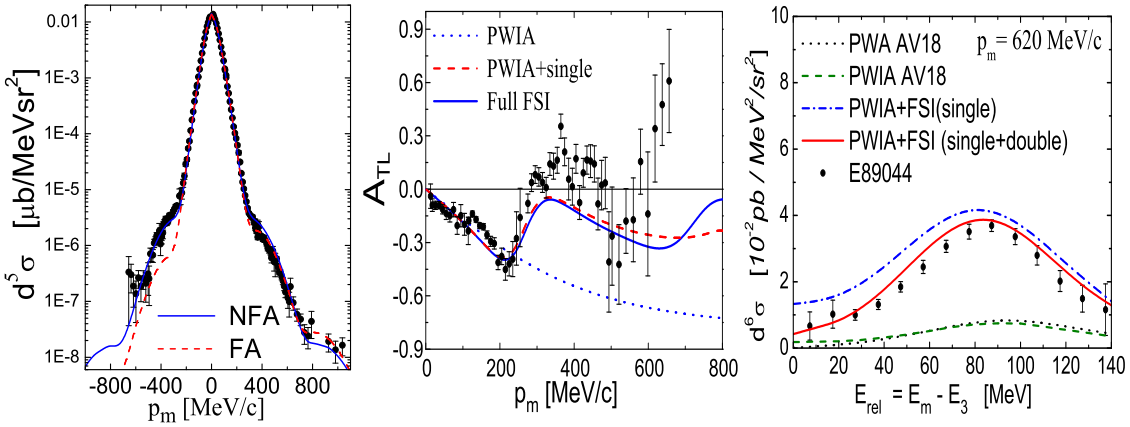

FIGURE 1. LEFT: the five-fold cross section $d^5\sigma \equiv d^5\sigma \times (dE'd\Omega'd\Omega_{p_1})^{-1}$ of the 2bbu channel $^3He(e,e'p)^2H$ calculated in GEA within the non factorized (NFA) and factorized (FA) approaches *vs* the missing momentum p_m. CENTER: the A_{TL} asymmetry. RIGHT: the six-fold cross section $d^6\sigma \equiv d^6\sigma \times (dE'd\Omega'd\Omega_{p_1}dE_m)^{-1}$ of the 3bbu channel plotted, at fixed value of p_m, *vs* the excitation energy E_{rel} of the two-nucleon system in the continuum. Experimental data from [10, 11] (After Ref. [9])

applied to a systematic calculation of the two-body (2bbu) and three-body (3bbu) break up channels of the $^3He(e,e'p)X$ reaction [4, 5] using realistic three-body wave functions [6, 7] and interactions [8]. In GEA the final state wave function has the following form (spin and isospin variables are omitted for ease of presentation)

$$\Psi_f(\mathbf{r}_1,\ldots\mathbf{r}_A) = \hat{\mathscr{A}} S_{GEA}(\mathbf{r}_1,\ldots\mathbf{r}_A) e^{-i\mathbf{p}_1\mathbf{r}_1} e^{-i\mathbf{P}_{A-1}\mathbf{R}_{A-1}} \Phi_{A-1}(\mathbf{r}_2,\ldots\mathbf{r}_A) \qquad (1)$$

where $S_{GEA} = \sum_{n=1}^{A-1} S_{GEA}^{(n)}$ takes care of the FSI; here, n denotes the order of multiple scattering, with the single scattering term (n=1) given by $S_{GEA}^{(1)}(\mathbf{r}_1,\ldots\mathbf{r}_A) = 1 - \sum_{i=2}^{A} \theta(z_i - z_1) e^{i\Delta_z(z_i-z_1)} \Gamma(\mathbf{b}_1 - \mathbf{b}_i)$, where $\Gamma(\mathbf{b}) = \sigma_{NN}^{tot}(1 - i\alpha_{NN}) \cdot exp[-\mathbf{b}^2/2b_0^2]/[4\pi b_0^2]$ is the usual Glauber profile function and $\Delta_z = (q_0/|\mathbf{q}|)E_m$, E_m being the removal energy related to the excitation energy of $A-1$. Note that when $\Delta_z = 0$, the usual GA is recovered. A fully non-factorized calculation (NFA) of the 2bbu and 3bbu channels has been recently performed [9] within a fully parameter free GEA approach. The results are shown in Fig. 1. It can be seen that in the 2bbu channel the factorized approximation (FA) is a poor one in the left region ($\phi = 0$, ϕ being the angle between the scattering and reaction planes) of the missing momentum, unlike what happens in the right region ($\phi = \pi$). The quantitative disagreement between theory and experiment is visualized in terms of the left-right asymmetry $A_{TL} = [d\sigma(\phi = 0^o) - d\sigma(\phi = 180^o)]/[d\sigma(\phi = 0^o) + d\sigma(\phi = 180^o)]$. As for the 3bbu channel shown in the same Figure, the differences between the FA and NFA amount at most at $10-15\%$. The results for the process $^4He(e,e'p)^3He$ are shown in Fig. 2. It can be seen that: i) the dip predicted by the PWIA is completely filled up by the FSI; ii) like the ^3He case, the difference between GA and GEA is not

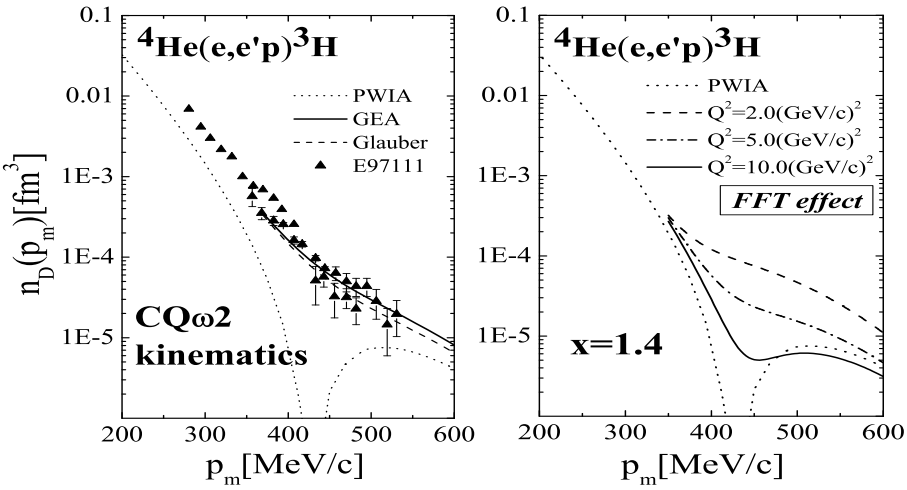

FIGURE 2. LEFT: the reduced cross section ($n_D(\mathbf{p}_m) = (d^5\sigma/d\Omega' dE' d\Omega_{p_1}) \times (\mathscr{K}\sigma_{ep})^{-1}$) of the process $^4He(e,e'p)^3H$ at perpendicular kinematics and $x \simeq 1.8$. The solid line shows the results within GEA, whereas the dashed curve corresponds to the conventional GA. Preliminary data from [12]. RIGHT: the reduced cross section at perpendicular kinematics for various values of Q^2 and $x \simeq 1.4$, calculated taking FFT effects [13] into account. Four-body wave functions from [14]. Experimental data from [17]. (After Refs. [15], [16] and [18])

very large; iii) an overall satisfactory agreement between theory and experiment is obtained. In Fig. 2 the results which take into account the finite formation time (FFT) of the proton are also shown. In [13] FFT effects have been implemented by explicitly considering the dependence of the NN scattering amplitude upon nucleon virtuality, leading to a replacement of $\theta(z_i - z_1)$, appearing in the Glauber profile, with $J(z_i - z_1) = \theta(z_i - z_1)\left(1 - \exp[-(z_i - z_1)/l(Q^2)]\right)$ where $l(Q^2) = Q^2/(xm_N M^2)$; here x is the Bjorken scaling variable and the quantity $l(Q^2)$ plays the role of the proton formation length, i.e. the length of the trajectory that the knocked out proton runs until it returns to its asymptotic form; the quantity M^2 is $M^2 = m^{*2} - m_N^2$ and since the formation length grows linearly with Q^2, at higher Q^2 the strength of the Glauber-type FSI is reduced by the damping factor $(1 - \exp[-(z_i - z_1)/l(Q^2)])$. It can be seen that at the JLAB kinematics ($Q^2 = 1.78\,(GeV/c)^2$, $x \sim 1.8$) FFT effects, as expected, are too small to be detected, but they can unambiguously be observed in the region $5 \leq Q^2 \leq 10\,(GeV/c)^2$ and x =1.4.

A(e, e′)X AND A(e, e′p)B PROCESSES OFF COMPLEX NUCLEI

Recently [19, 20, 21] the ground state properties (energy, density and momentum distributions) of closed shell and sub-shell nuclei have been obtained by a cluster expansion approach based upon a correlated wave function

$$\psi_o(\mathbf{r}_1, \mathbf{r}_2, ..., \mathbf{r}_A) = \hat{F}(\mathbf{r}_1, \mathbf{r}_2, ..., \mathbf{r}_A)\, \phi_o(\mathbf{r}_1, \mathbf{r}_2, ..., \mathbf{r}_A) \qquad (2)$$

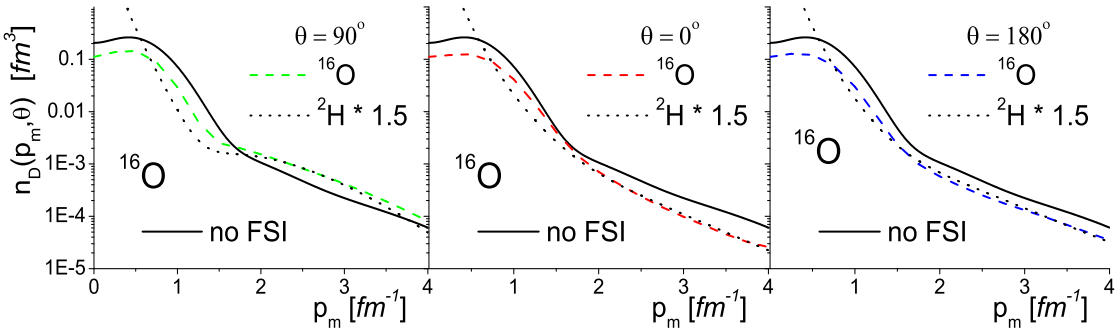

FIGURE 3. The distorted missing momentum distributions of ^{16}O at various angles (dashes) compared with the rescaled deuteron distorted momentum distribution at the same angles (dots). The full line represents the undistorted momentum distribution. Wave functions from Ref. [19]. (After Ref. [22])

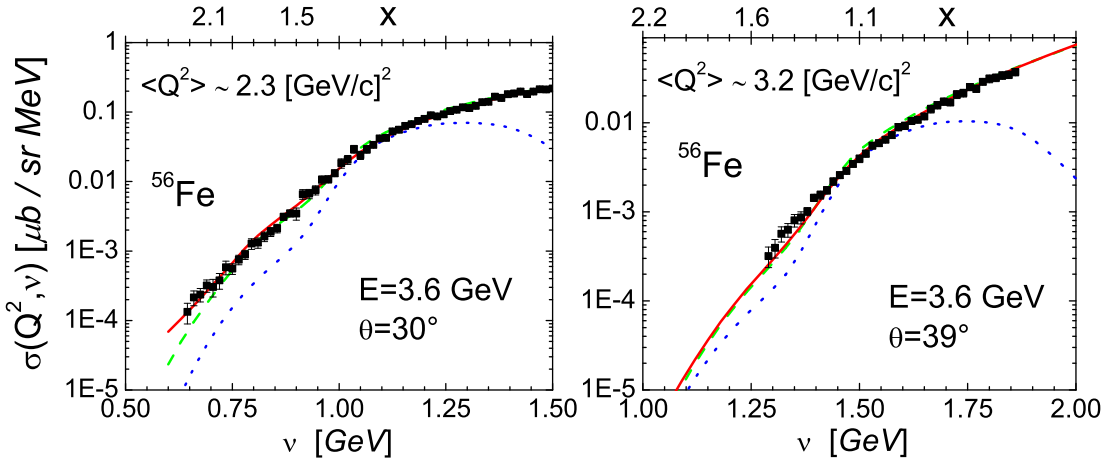

FIGURE 4. The experimental inclusive cross section $^{56}Fe(e,e')X$ [25] compared with theoretical calculations which include SRC [23] and FSI [24]. ***Dotted lines***: PWIA; ***dashed lines***: PWIA + FSI of the correlated struck nucleon with the correlated partner; ***full lines***: the same as ***dashed lines*** plus the FSI of the shell model struck nucleon with the mean field of the $(A-1)$ spectator. (After Ref. [26])

where ϕ_o is a *mean-field* wave function and

$$\hat{F} = \hat{S}\prod_{i<j}\hat{f}_{ij} = \hat{S}\prod_{i<j}\sum_{n=1}^{N} f^{(n)}(r_{ij})\,\hat{\mathcal{O}}_{ij}^{(n)} \tag{3}$$

is a symmetrized *correlation* operator generating NN correlations according to the modern forms of the two-nucleon interaction, i.e. [8] $V(\hat{i},j) = \sum_{n=1}^{N} v^{(n)}(r_{ij})\,\hat{\mathcal{O}}_{ij}^{(n)}$ where the state-dependent operator is $\hat{\mathcal{O}}_{ij}^{(n)} = \left[1, \sigma_i\cdot\sigma_j, \hat{S}_{ij}, (\mathbf{S}\cdot\mathbf{L})_{ij}, L^2, L^2\sigma_i\cdot\sigma_j, (\mathbf{S}\cdot\mathbf{L})_{ij}^2, ..\right]\otimes\left[1, \tau_i\cdot\tau_j\right]$. The ground state properties have been obtained by cluster expanding the

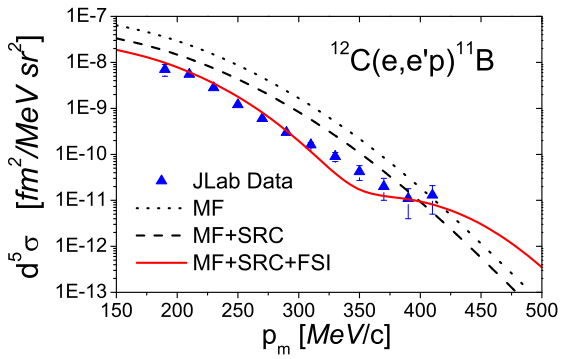

FIGURE 5. The preliminary Jlab data [27] on of the exclusive reaction $^{12}C(e,e'p)^{11}B$ compared with Mean Field (*MF*) predictions (*dots*) and with the predictions of *MF + SRC* (*dashes*) and *MF+SRC + FSI* (*full*); $d^5\sigma \equiv d^5\sigma \times (d\Omega' d\Omega_{p_1} dE_{p_1})^{-1}$. (After Ref. [28])

appropriate density matrices. Using the wave function parameters which minimize the ground state energy and GEA, a realistic approach to SRC and FSI is achieved. In Fig. 3 the distorted momentum distributions for ^{16}O are shown and compared with the distorted momentum distribution of the deuteron, finding, at high values of the missing momentum, an amazing similarity between them, as in the case of the undistorted momentum distributions [23]. The inclusive cross section calculated by separately considering FSI in the correlated pair and in the $(A-1)$ mean field [23, 24] are presented in Fig. 4, which clearly demonstrates the relevant role played by FSI in the SRC pair. A comparison between preliminary Jlab data on the exclusive process $^{12}C(e,e'p)^{11}B$ and theoretical calculations based upon correlated wave functions and Glauber FSI, are presented in Fig. 5.

THE TENSOR FORCE AND pn/pp CORRELATIONS

The role of the tensor force in producing a substantial difference between *pn* and *pp* two-nucleon momentum distributions in few-body systems and light nuclei ($A \leq 8$), has been recently demonstrated [29, 30] using state-of-the-art realistic nuclear wave functions obtained within the Variational Monte Carlo (VMC) approach [7]. The same conclusion for complex nuclei ($12 \leq A \leq 40$) has been reached in [21] within the approach of Ref. [19]. The two-body Momentum Distribution is ($\mathbf{k}_{rel} = (\mathbf{k}_1 - \mathbf{k}_2)/2$, $\mathbf{K}_{CM} = (\mathbf{k}_1 + \mathbf{k}_2)$)

$$n(\mathbf{k}_{rel}, \mathbf{K}_{CM}) = \frac{1}{(2\pi)^6} \int d\mathbf{r} d\mathbf{r}' d\mathbf{R} d\mathbf{R}' e^{-i\mathbf{K}_{CM}\cdot(\mathbf{R}-\mathbf{R}')} e^{-i\mathbf{k}_{rel}\cdot(\mathbf{r}-\mathbf{r}')} \rho^{(2)}(\mathbf{r}, \mathbf{r}'; \mathbf{R}, \mathbf{R}')$$

where $\rho^{(2)}(\mathbf{r}, \mathbf{r}'; \mathbf{R}, \mathbf{R}')$ is the non-diagonal two-body density matrix. The relative (integrated over **R**) density matrix $\rho^{(2)}(\mathbf{r}_{rel})$, the quantity $n(\mathbf{k}_{rel}, \mathbf{K}_{CM} = 0)$, describing back-to-back nucleons, and the effects from the tensor force on $n_{pN}(\mathbf{k}_{rel}, \mathbf{K}_{CM} = 0)$, characterized by the ratio $R_{pN} = n_{pN}(k_{rel}, 0) \,/\, n_{pN}^{central}(k_{rel}, 0)$, are shown in Fig. 6. In ref. [21]

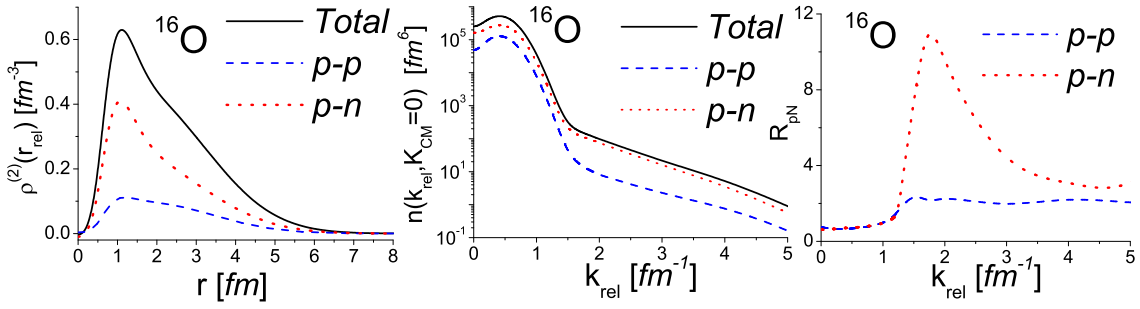

FIGURE 6. LEFT: the ^{16}O relative (integrated over **R**) diagonal two-body density distribution. CENTER: the two-body momentum distribution for $\mathbf{K}_{CM} = 0$. RIGHT: the ratio $R_{pN} = n_{pN}(k_{rel},0) \,/\, n_{pN}^{central}(k_{rel},0)$. (After Refs. [21, 31]

TABLE 1. The pp and pn percentage probability (Eq. (4)) evaluated in the momentum range shown in square brackets.

A	P_{pp} (%) $[0,\infty]$	P_{pn} (%) $[0,\infty]$	P_{pp} (%) $[1.5,3.0]$	P_{pn} (%) $[1.5,3.0]$
4	19.7	81.3	2.9	97.1
12	30.6	69.4	13.3	86.7
16	29.5	70.5	10.8	89.2
40	31.0	69.0	24.0	76.0

the percentage probability to find in the nucleus a pN pair defined by

$$P_{pN} = \frac{\int_a^b dk_{rel}\, k_{rel}^2\, n_{pN}(k_{rel},0)}{\int_a^b dk_{rel}\, k_{rel}^2\, \left(n_{pp}(k_{rel},0) + n_{pn}(k_{rel},0)\right)}\,. \tag{4}$$

has been calculated. The results are shown in Table 1. It can be seen that, in agreement with the result of Ref. [29], when the integration runs over the whole range of k_{rel}, P_{pN} is proportional to the percentage of pN pairs, whereas the integration over the correlation region leads to a percentage of pn pairs much larger than that of the pp pairs, which is clear consequence of the effects of the tensor force acting between a proton and a neutron. We found that in medium-weight nuclei $P_{pp} \simeq 10\%$ and $P_{pn} \simeq 90\%$ in agreement with the findings of Ref. [32] obtained from the reactions $^{12}C(e,e'pn)$ and $^{12}C(e,e'pp)$. The effects of various CM motion configurations on the value of P_{pN} are being investigated [31].

SRC AND HIGH-ENERGY SCATTERING

Nowadays the interpretation of high precision particle-nucleus and nucleus-nucleus scattering experiments at high energies, aimed at investigating the state of matter at short distances, should require in principle also a consideration of possible effects from NN

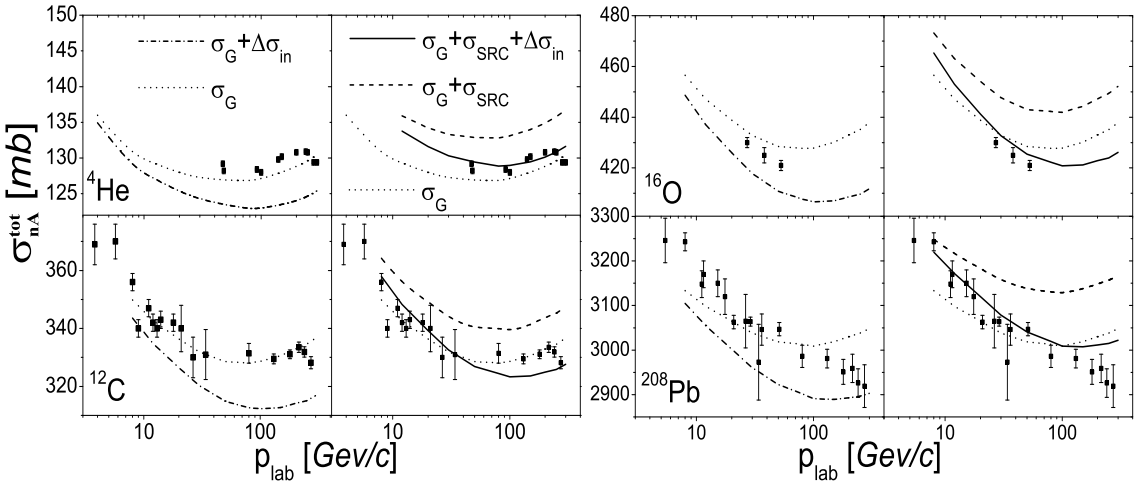

FIGURE 7. The neutron-nucleus total cross section at high energies. LEFT PANELS: Glauber (σ_G; *dots*) and Glauber plus Gribov inelastic shadowing ($\sigma_G + \Delta\sigma_{in}$; *dot-dashes*). RIGHT PANELS: Glauber (σ_G; *dots*), Glauber plus SRC ($\sigma_G + \sigma_{SRC}$; *dashes*) and Glauber plus SRC plus Gribov inelastic shadowing ($\sigma_G + \sigma_{SRC} + \Delta\,\sigma_{in}$; *full*). For references to the experimental data see [36]. (After Ref. [33])

correlations, which are usually disregarded in Glauber-type approaches which consider only the first term (*single density approximation*) of the exact expansion

$$|\Psi(\mathbf{r}_1,...,\mathbf{r}_A)|^2 = \prod_{j=1}^{A}\rho(\mathbf{r}_j) + \sum_{i<j=1}^{A}\Delta(\mathbf{r}_i,\mathbf{r}_j)\prod_{k\neq(ij)}^{A}\rho_1(\mathbf{r}_k) + \ldots \tag{5}$$

where $\Delta(\mathbf{r}_i,\mathbf{r}_j) = \rho_2(\mathbf{r}_i,\mathbf{r}_j) - \rho_1(\mathbf{r}_i)\,\rho_1(\mathbf{r}_j)$, yielding $\int d\mathbf{r}_2\Delta(\mathbf{r}_1,\mathbf{r}_2) = 0$.

In Ref. [33, 34] the elastic, quasi-elastic and total nucleon-nucleus cross sections at high energies have been calculated within Glauber approach taking also into account all correlation terms in the expansion (5) using density matrices from Ref. [19]. The effects of correlations and Gribov inelastic shadowing [35] on the total neutron-nucleus cross section, which has been measured with high precision, are given by

$$\sigma_{tot} = 2Re\int d\mathbf{b}\left[1 - \int\prod_{j=1}^{A}d\mathbf{r}_j\,[1-\Gamma(\mathbf{b}-\mathbf{s}_j)]\cdot|\Psi_0(\mathbf{r}_1,...,\mathbf{r}_A)|^2\right] \tag{6}$$

The results of calculations are shown in Fig. 7, which clearly exhibits the role of SRC.

CONCLUSIONS

We have shown that a large wealth of different experimental data concerning medium and high energy scattering off nuclei can be interpreted within a framework which includes a proper treatment of initial state short range correlations and final state interactions. In the former, tensor and isospin-tensor correlations appear to be the essential

ingredients for a correct description of one- and two-nucleon momentum distributions both in few-body systems and complex nuclei. As for the latter, Glauber multiple scattering and the generalized eikonal approximation appear to be a satisfactory frameworks for the description of the final state interaction. At high values of the missing momentum both the undistorted and distorted one-nucleon and relative momentum distributions strikingly resemble the same quantities pertaining to deuteron. Finally, according to our results, the effects of SRC on high energy scattering processes, if properly treated, should not be overlooked.

REFERENCES

1. R. Subedi *et al.*, Science 320 (2008) 1476
2. C. Ciofi degli Atti, E. Pace and G. Salmè Phys. Rev. C43 (1991) 1193
3. M. M. Sargsian, T. V. Abrahamyan, M. I. Strikman and L. L. Frankfurt, Phys. Rev. C71 (2005) 044614.
4. C. Ciofi degli Atti and L.P. Kaptari, Phys. Rev. C71 (2005) 024005; Phys. Rev. Lett. 95 (2005) 052502
5. R. Schiavilla, O. Benhar, A. Kievsky, L. E. Marcucci and M. Viviani, Phys. Rev. C72 (2006) 064003
6. A. Kievsky, S. Rosati and M. Viviani, Nucl. Phys. A551 (1993) 241
7. J. Carlson and R. Schiavilla, Rev. Mod. Phys. 70 (1998) 743
8. R.B. Wiringa, V. G. Stokes and R. Schiavilla, Pys. Rev. C51 (1995) 38
9. C. Ciofi degli Atti and L. P. Kaptari, Phys. Rev. Lett. 100 (2008) 122301 and *to appear*
10. M. M. Rvachev *et al.*, Phys. Rev. Lett. 94 (2005) 192302
11. F. Benmokhtar *et al.*, Phys. Rev. Lett. 94 (2005) 082325
12. B. Reitz *et al.*, Eur. Phys. J. A S19 (2004) 165
13. M. A. Braun, C. Ciofi degli Atti and D. Treleani, Phys. Rev. C62 (2000) 034606
14. H. Morita, Y. Akaishi, O. Endo and H. Tanaka, Prog. Theor. Phys. 78(1987)1117; H. Morita, Y. Akaishi and H. Tanaka, Prog. Theor. Phys. 79 (1988) 1279
15. C. Ciofi degli Atti, L. P. Kaptari and H. Morita, Nucl. Phys. A782(2007)191c.
16. H. Morita, M. Braun, C. Ciofi degli Atti and D. Treleani, Nucl. Phys. A699 (2002) 328c
17. B. Reitz *et al.*, Eur. Phys. J. A S19 (2004) 165
18. C. Ciofi degli Atti, L. P. Kaptari, H. Morita in "Few Body Systems", *in press* arXiv:0803.1162
19. M. Alvioli, C. Ciofi degli Atti, H. Morita, Phys. Rev. C72 (2005) 054310
20. M. Alvioli, C. Ciofi degli Atti, H. Morita, Fizika B 13 (2004) 585
21. M. Alvioli, C. Ciofi degli Atti, H. Morita, Phys. Rev. Lett 100 (2008) 162503
    M. Alvioli, C. Ciofi degli Atti and H. Morita, in *Science and Supercomputing in Europe - Report 2007*; *P. Alberigo, G. Erbacci and F. Garofalo Editors*, Bologna (2007); arXiv:0709.3989v1
22. M. Alvioli, C. Ciofi degli Atti, H. Morita, V. Palli, *to appear*
23. C. Ciofi degli Atti and S. Simula, Phys. Rev. C53 (1996) 1689
24. C. Ciofi degli Atti and S. Simula, Phys. Lett. B319 (1993) 23
25. D. B. Day at al., Phys. Rev. Lett. 59 (1987) 427
26. C. Ciofi degli Atti, C. B. Mezzetti, *to appear*
27. R. Shneor *et al*, Phys. Rev. Lett. 99 (2007) 072501; and *private communication*
28. M. Alvioli, C. Ciofi degli Atti and H. Morita, *in preparation*
29. R. Schiavilla, R. B. Wiringa, S. C. Pieper and J. Carlson, Phys. Rev. Lett. 98 (2007) 132501
30. R. B. Wiringa, R. Schiavilla, S. C. Pieper and J. Carlson, arXiv:0806.1718v1
31. M. Alvioli, C. Ciofi degli Atti and S. Scopetta, *to appear*
32. E. Piasetzky, M. Sargsian, L. Frankfurt, M. Strikman and J. W. Watson Phys. Rev. Lett. 97 (2006) 162504.
33. M. Alvioli, Ciofi degli Atti, I. Marchino, H. Morita and V. Palli, arXiv:07053613
34. M. Alvioli, Ciofi degli Atti and V. Palli, *in preparation*
35. V. A. Karmanov, L. A. Kondratyuk, JETP Lett. 18 (2008) 162503
36. P. V. Murthy, C. A. Ayre, H.R. Gustafson, L. W. Jones and M. J. Longo, Nucl. Phys. B92 (1975) 269